Vol. 168, No. 1, 1990 BIOCHEMICAL AND BIOPHYSICAL RESEARCH COMMUNICATIONS
April 16, 1990 Pages 364-371

IMPROVED RESOLUTION OF THE INITIAL FAST PHASE OF HEAVY SARCOPLASMIC RETICULUM Ca^{2+} UPTAKE BY Ca^{2+}:ANTIPYRYLAZO III DUAL-WAVELENGTH SPECTROSCOPY

James S.C. Gilchrist, Sidney Katz and, Angelo N. Belcastro*

Faculties of Graduate Studies, Pharmaceutical Sciences and, Medicine and Education, University of British Columbia, Vancouver, British Columbia, Canada V6T 1W5

Received March 5, 1990

SUMMARY: The effect of ATP upon difference absorbance due to Ca^{2+} and Mg^{2+} complexation with the metallochromic dye, Antipyrylazo III (AP III), was investigated. At divalent cation concentrations appropriate for Sarcoplasmic Reticulum Ca^{2+} transport, wavelengths (>670nm) were found whereupon the addition of up to 1mM nucleotide did not alter divalent cation:AP III difference absorbance. At these sample wavelengths an initial rapid uptake of Ca^{2+} by Heavy SR (HSR) was clearly resolved by dual wavelength spectroscopy of Ca^{2+}:dye difference absorbance. Elimination of ATP interference of Ca^{2+}:AP III absorbance by Mg^{2+} elevation (3-10mM) was shown to be an inappropriate general strategy for AP III spectroscopic studies of HSR Ca^{2+} transport due to Mg^{2+} inhibition of ryanodine receptor mediated Ca^{2+} release.

The Sarcoplasmic Reticulum (SR) of skeletal and cardiac muscle forms a critical link during excitation-contraction coupling through the rapid release and re-uptake of Ca^{2+} into and from, respectively, the myoplasmic space (1). The regulation of Ca^{2+} fluxes by isolated SR vesicles has been conveniently studied, in vitro, utilising dual-wavelength spectroscopy of Ca^{2+} sensitive metallochromic dyes (Murexide, Arsenazo III, Antipyrylazo III) (2,3,4). In particular, Antipyrylazo III (AP III), is an effective Ca^{2+} probe for the study of Heavy SR (HSR) Ca^{2+} uptake (4) and Ca^{2+} release induced by nucleotides (5), caffeine (6), sulphydryl modification (7), Ca^{2+} (8) and various drugs (9,10). Ca^{2+} binds to AP III with a 1:2 stoichiometry (11) and the Ca^{2+}:AP III complex (CaD_2) exhibits linear absorbance over a Ca^{2+} concentration range (10-60μM) that is appropriate for such studies. A disadvantage of this method is the substantial artifactual absorbance shift that is observed at the customary 720-790nm wavelength pair upon the addition of high ATP (>500μM) in the presence of low Mg^{2+} (6,8). Consequently, the initial phase of Ca^{2+} accumulation has been poorly resolved when SR Ca^{2+} transport is initiated by the addition of millimolar ATP. The problem of ATP absorbance artifacts was circumvented by the inclusion of high Mg^{2+} (10mM) in assay buffers (11) although this strategy may not be advantageous due to Mg^{2+} inhibition of SR Ca^{2+}-ATPase (EC; 3.6.1.38) and ryanodine receptor mediated Ca^{2+} release (12,13). In

*Correspondence: A. Belcastro, Ph.D., Laboratory of Cellular Physiology and Exercise, 6081 University Boulevard, University of British Columbia, Vancouver, British Columbia, Canada, V6T 1W5.

Abbreviations: SR, Sarcoplasmic Reticulum; HSR, Heavy SR; AP III, Antipyrylazo III; PIPES, 1,4,-piperazinediethanesulphonic acid; EGTA; [ethylenebis(oxyethylenitrilo)]tetraacetic acid; PC, creatine phosphate; CPK, creatine phosphokinase; SDS, sodium dodecyl sulphate; K_{CaD}, Ca^{2+}:AP III dissociation constant; εCaD_2, Ca^{2+}:AP III molar extinction coefficient.

0006-291X/90 $1.50

this report we document the effect of ATP upon difference absorbance (ΔA) due to formation of AP III:divalent cation (Ca^{2+} and Mg^{2+}) complexes. Within a range of Ca^{2+}, Mg^{2+} and, ATP appropriate for the study of HSR Ca^{2+} transport, in vitro, we demonstrate that selection of new wavelength pairs eliminates the ATP dependent artifact with improved resolution of the initial rapid phase of HSR Ca^{2+} transport.

MATERIALS AND METHODS

Spectroscopy: Antipyrylazo III (AP III) was purchased from Sigma (Sigma Chemical Co., St. Louis, MO) and purified by double re-crystallisation as described (14). Double beam difference spectra (between 640nm and 790nm) and dual-wavelength records of Ca^{2+} transport were obtained using a SLM Aminco DW2C spectrophotometer on-line with a SLM Aminco MIDAN II kinetic processor/controller. The optical chopper speed was 270 Hz with a monochromator bandpass set to 3nm. The light path was 1cm (quartz cuvettes) and automatic baseline correction was performed for each dye:ligand difference spectral record. The basic cuvette (3ml) solution for spectral records contained 300mM sucrose, 150mM KCl, 20mM PIPES, 50μM AP III (pH 7.0) supplemented with concentrated stocks of Mg.ATP, Mg^{2+} and, Ca^{2+} (prepared in the basic medium) as described in the figure legends. All cuvette solutions were thermostatically controlled (27°C) and continually mixed with a magnetic flea stirring accessory.

Calculation of Dissociation Constants: The molar extinction coefficients of the Ca^{2+} free AP III (εD) and the Ca^{2+} bound AP III (εCaD_2) were obtained in the presence of 200μM EGTA and 2mM AP III, respectively, using procedures described for Arsenazo III (15). The measuring wavelength was 685nm and values of εD=0.7 ($mM^{-1}.cm^{-1}$) and εCaD_2=8.33 and 7.14 ($mM^{-1}.cm^{-1}$) at zero and 1mM Mg^{2+}, respectively, were calculated. $[CaD_2]$ was obtained from $\Delta A=(\varepsilon CaD_2-2\varepsilon D).[CaD_2]$ (16) and $Ca_f=Ca_t-[CaD_2]$ where Ca_f=free Ca^{2+} and Ca_t=total Ca^{2+}. Apparent first order dissociation constants (K'_{CaD}) for CaD_2 in the absence and presence of 1mM Mg^{2+} were obtained by Ca^{2+} titration of 50μM AP III. The value was calculated from the negative reciprocal abscissa intercept obtained from double reciprocal plots of ΔA vs Ca_f. Each plot was a linear least-squares fit to the data. Second order dissociation constants (K''_{CaD}) were obtained, as described (17), from the relation $K''_{CaD}=Ca_f.(D_t-2CaD_2)^2/CaD_2$ where D_t is the total [AP III] (50μM).

HSR Isolation: HSR vesicles were isolated from rabbit fast twitch skeletal muscle essentially as described (18). Protein banding in the 38% to 40% region of sucrose density gradients was finally resuspended to about 35mg.ml^{-1}, rapidly frozen in liquid N_2 and, stored at -80°C until required.

HSR Calcium Transport: 1mg.ml^{-1} HSR vesicles were pre-incubated for 1 minute in media containing 300mM sucrose, 150mM KCl, 20mM PIPES, 70μM Ca^{2+}, 50μM AP III (pH 7.0, 27°C) and, various concentrations of Mg^{2+} as indicated in the figure legends. Ca^{2+} uptake was initiated by addition of stock Mg.ATP to a final concentration of 1mM. Mg.ATP and other reagents were introduced to the sample compartment with a Unimetrics microlitre syringe through a customised diaphragm that completely excluded the entry of external light. When required, ATP regeneration was supported by the inclusion of 5mM creatine phosphate (PC) and 12.5 units.ml^{-1} creatine phosphokinase (CPK: EC 2.7.3.2; from rabbit skeletal muscle) during pre-incubation. PC and CPK were purchased from Sigma.

Miscellaneous: Protein concentration was determined by the method of Lowry et al. (19) modified by the inclusion of 1% SDS to solubilise membrane proteins. All regeants used were of the highest grade available. Free ion concentrations were calculated using a computer program, as described (20).

RESULTS AND DISCUSSION

The CaD_2 difference spectrum between 640nm and 790nm is shown in Figure 1A (trace a). The observation of maxima (λ_{max}) at 652nm and 716nm with an isosbestic point at the 790nm reference wavelength is consistent with previous reports (14). In addition, good agreement between apparent first order (K'_{CaD}=257μM) and second order (K''_{CaD}=24789μM^2) dissociation constants, fixed by the relationship $K'_{CaD}=K''_{CaD}/2D$ where D is the total dye concentration (16), was obtained. Addition of Mg^{2+} to sample cuvette solutions containing 50μM Ca^{2+} decreased dye:ligand ΔA particularly at wavelengths above 700nm with formation of a single λ_{max} at 685nm (Fig. 1A). Part of the Mg^{2+} effect is via a reduction of the CaD_2 stability constant with formation of a 1:1 complex (MgD) with the pure dye

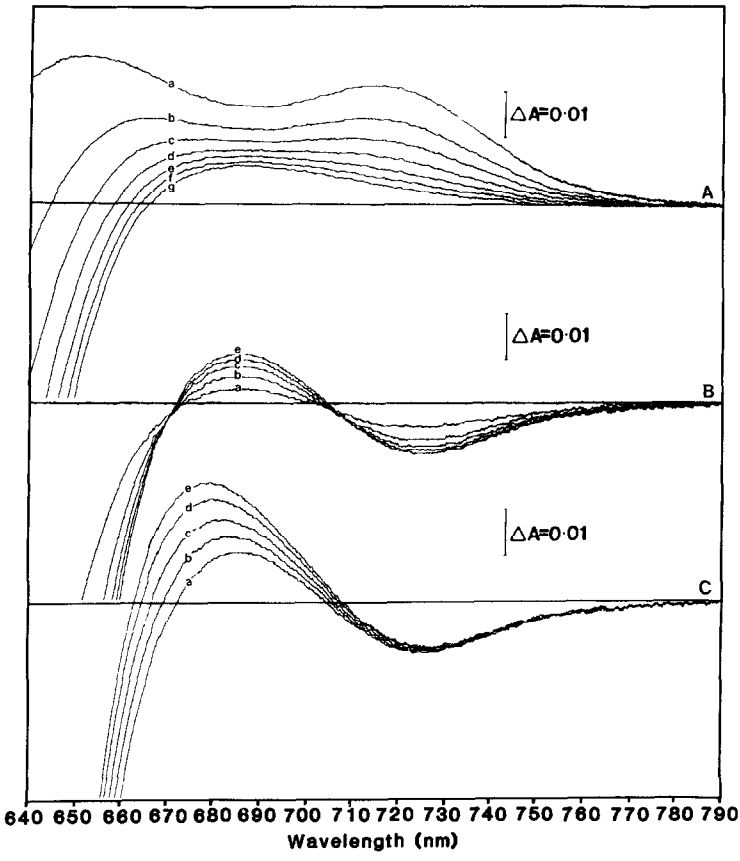

Figure 1: Double beam spectroscopy of AP III:divalent cation ΔA spectra. (A). Effect of Mg^{2+} upon difference spectra in the presence of Ca^{2+}. Trace a is the Ca^{2+}:AP III difference spectrum obtained with 50μM Ca^{2+} and 50μM AP III. Mg^{2+} was added in 500μM increments (traces b to g) to a final concentration of 3mM. (B). Mg^{2+}:AP III difference spectra. Mg^{2+} was added in 1mM increments (traces a to e) to 5mM (trace e). (C) Effect of Tris-ATP (traces b to e) upon difference spectra in the presence of 5mM Mg^{2+} (trace a). Nucleotide was added in 250μM increments to a final concentration of 1mM. Both reference and sample cuvettes contained basic solution (see **Methods**). Ca^{2+}, Mg^{2+} and nucleotide were added to the sample cuvette from stock (2.5mM, 100mM and 50mM, respectively) prepared in basic solution. Spectra (between 640 and 790 nm) were obtained after baseline subtraction. Scales for ΔA are as indicated with positive and negative absorbance positioned above and below, respectively, the horizontal baseline in each figure.

(21). In agreement with previous reports (14,16) 1mM Mg^{2+} increased K'_{CaD} and K''_{CaD} 1.24 and 1.26 fold, respectively (data not shown). However, isosbestic points for the MgD spectra were recorded at 670nm and 705nm with an observed λ_{max} at 685nm (Fig. 1B) that coincides with λ_{max} recorded at 3mM Mg^{2+} in the presence of Ca^{2+} (Fig. 1A). This is contrary to earlier reports (14) where, at higher ionic strength (500mM KCl), MgD absorbance above 660nm was not detected. The MgD difference spectrum was itself modified by the addition of ATP (tris salt) with elevated absorbance below 720nm and shift of λ_{max} to 675nm (Fig. 1C). However, addition of tris.ATP (to 5mM) to sample cuvette solutions with zero added Ca^{2+} or 200μM EGTA did not result in detectable absorbance above 600nm (data not shown).

In the presence of both Ca^{2+} and Mg^{2+}, nucleotide addition altered the spectral waveform in a manner that was dependent upon the relative proportion of divalent cation. At high Ca^{2+} (50μM) and 1mM Mg^{2+}, Mg.ATP addition decreased ΔA above 700nm with small effects at 670nm (Fig. 2A). At low Ca^{2+}

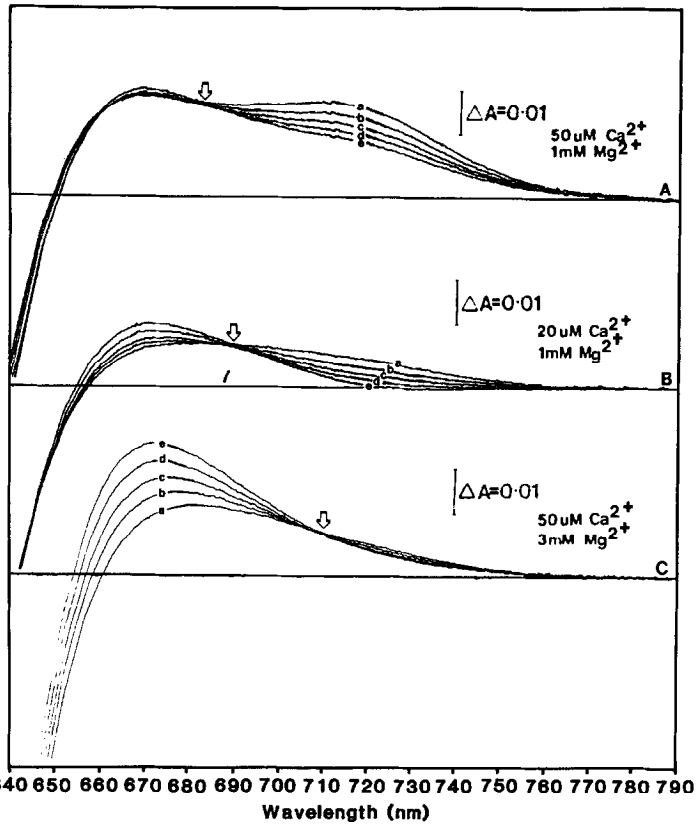

Figure 2: Effect of Mg.ATP upon AP III:divalent cation difference spectra. Nucleotide was added in 250μM increments (traces b-c) to 1mM final concentration (trace e) in the presence of (A). 50μM Ca^{2+}, 1mM Mg^{2+} (B). 20μM Ca^{2+}, 1mM Mg^{2+} (C). 50μM Ca^{2+}, 3mM Mg^{2+}. All other conditions and figure descriptions are as described in the legend to Figure 1.

(20μM) and 1mM Mg^{2+} the addition of Mg.ATP decreased and increased ΔA at 700nm and 685nm respectively (Fig. 2B). Nucleotide addition with both elevated Mg^{2+} and Ca^{2+} modified the ΔA spectra (Fig. 2C) in a manner similar to that observed in the absence of added Ca^{2+} (Fig. 1C). Within the range of divalent cations defined by Fig. 2 the addition of up to 1mM Mg.ATP led to the appearance of cross-over points (open arrows) which intersected the spectra obtained prior to the addition of nucleotide. The cross-over point is not a true isosbestic point since the position was dependent upon the relative concentrations of divalent cation. Spectral modification was similar with tris-ATP addition although definition of the cross-over point was enhanced by Mg.ATP.

Nucleotide modification of divalent cation:dye ΔA spectra (Figs. 1 and 2) was complex and may arise, partly, from ATP buffered redistribution of bound and free divalent cation. The basis for the curious nucleotide elevation of ΔA at lower wavelengths (Fig. 1C and Fig.2) and it's dependence upon relative divalent cation concentration is unclear. However, observation of cross-over points is largely attributable to this phenomenon. Nucleotide elevation of absorbance at 670-680nm poorly correlated with any bound or free ligand species. Although marked effects were observed at high Mg^{2+}, nucleotide (tris or Mg^{2+} salt) addition in the presence of less than 0.5mM Mg^{2+} reduced ΔA at these wavelengths. The formation of cross-over points was also observed in the presence of creatine phosphate at slightly different wavelengths (data not shown).

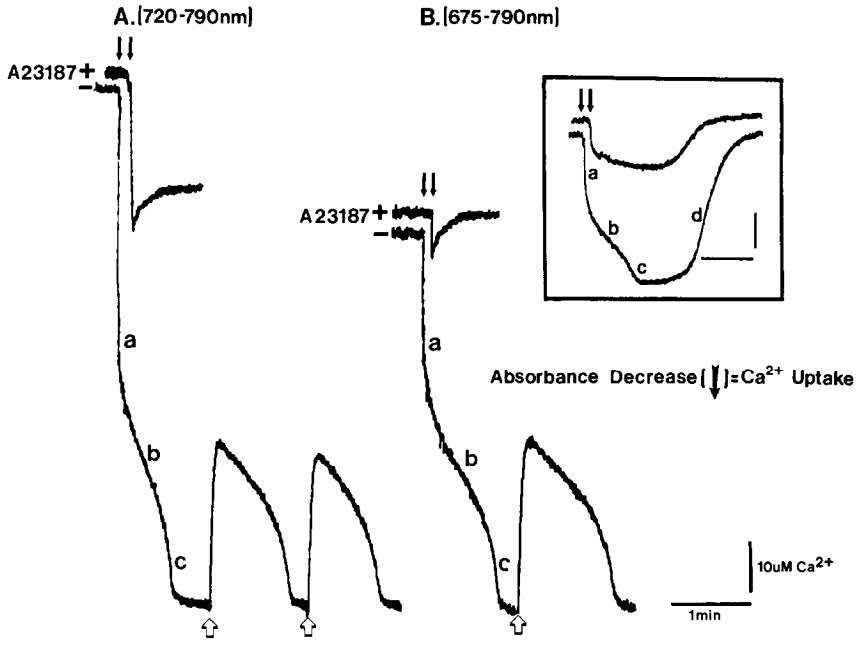

Figure 3: Effect of wavelength pair alteration upon dual-wavelength spectroscopic resolution of initial Ca^{2+} uptake by native HSR vesicles. Wavelength pairs were (A). 720-790nm and (B). 675-790nm. Ca^{2+} uptake was initiated by the rapid addition of 1mM Mg.ATP (solid arrows) in the presence of 1mM Mg^{2+}, 12.5 units.ml^{-1} CPK and, 5mM PC under conditions otherwise described in **Methods**. In both A and B vesicles were pre-incubated for 1 minute in the presence (+) or absence (-) of the Ca^{2+} ionophore, A23187 (10μM), prior to the addition of Mg.ATP. At the indicated times (open arrows) Ca^{2+} release was induced by the direct addition of 3μM Ca^{2+} to the cuvette. Downward excursions of the traces (absorbance decrease) denote Ca^{2+} uptake and upward excursions (absorbance increase) denote Ca^{2+} release. The scales for time (abscissa) and ΔCa^{2+} (ordinate) are as indicated. The component phases of uptake and release of Ca^{2+} are indicated on the traces (see text for explanation).

Inset: Shows the resolution of initial Ca^{2+} uptake at 682.5-790nm wavelength pair compared to Ca^{2+}-ATPase inhibition by Quercetin. Vesicles were pre-incubated in the presence (+) and absence (-) of 100μM Quercetin under conditions described above except for the absence of ATP regeneration. 1mM Mg.ATP addition (solid arrows) initiated Ca^{2+} uptake. The vertical and horizontal bars denote scales for ΔCa^{2+} and time with the same dimensions as for A and B.

The appropriateness of the divalent cation and nucleotide concentrations defined by Figs. 2A and 2B for the study of HSR Ca^{2+} transport, by dual-wavelength spectroscopy, is convenient as sample wavelengths could be set to cross-over points with elimination of ATP induced artifacts upon initiation of Ca^{2+} uptake with greater than 500μM nucleotide. Earlier, AP III:Ca^{2+} dual-wavelength spectroscopy studies of HSR Ca^{2+} transport supported by ATP regeneration suggested that only a slow phase initiated Ca^{2+} uptake when a 720nm sample wavelength was employed (6,8). However, resolution of initial Ca^{2+} uptake in these studies was obscured by nucleotide reduction of ΔA. In Fig. 3A the decrease in ΔA due to ATP was estimated by pre-incubation of HSR vesicles (1mg.ml^{-1}) with the Ca^{2+} ionophore A23187. Addition of 1mM Mg.ATP (solid arrows), reduced ΔA by 0.008 to 0.009 absorbance units consistent with the decrease observed in the absence of protein (see Fig. 2A). After subtraction of the ΔA artifact a substantial residual component of the rapid decrease in ΔA was observed in the absence of ionophore. In Fig. 3B Mg.ATP addition to HSR, pre-incubated with A23187, was without effect upon ΔA at 675nm in accord with Fig. 2A. At this sample wavelength Ca^{2+} uptake was clearly resolved into 3 kinetically distinguishable phases: a fast initial phase (a, >650nmol.mg^{-1}.min^{-1}); a slow secondary phase (b,

40nmol.mg^{-1}.min^{-1}) and; an intermediate tertiary phase (c, 85nmol.mg^{-1}.min^{-1}). After accumulation of essentially all extralumenal Ca^{2+} (including ~10μM contaminating Ca^{2+}) a steady state was reached. Repetitive addition of 3μM free Ca^{2+} (open arrows) to the medium triggered a rapid release of intralumenal Ca^{2+} (35nmol.mg^{-1}) consistent with earlier reports (3,6,8). The secondary and tertiary phases of uptake have been attributed to Ca^{2+} release channel opening and closing, respectively, and are modified by initial extravesicular Ca^{2+} load (8). The fast phase, however, appeared to be relatively independent of Ca^{2+} load (data not shown). The initial rapid phase of Ca^{2+} uptake by HSR may, therefore, involve rapid intralumenal binding of Ca^{2+} to calsequestrin as suggested (22,23). Initial rapid uptake of Ca^{2+} was, similarly, resolved in the absence of ATP regeneration (inset Fig. 3). With earlier such studies (5,12) the initial rapid uptake of Ca^{2+} was inferred from the large spontaneous release of Ca^{2+} (phase d, inset Fig. 3) attributed to ATP depletion (12). Ca^{2+}-ATPase inhibition by 100μM Quercetin (10) produced only small initial CaD_2 absorbance changes as expected. Therefore, the large initial ΔA decrease upon addition of Mg.ATP (phase a) represents a rapid uptake of Ca^{2+} the magnitude of which can be assessed directly.

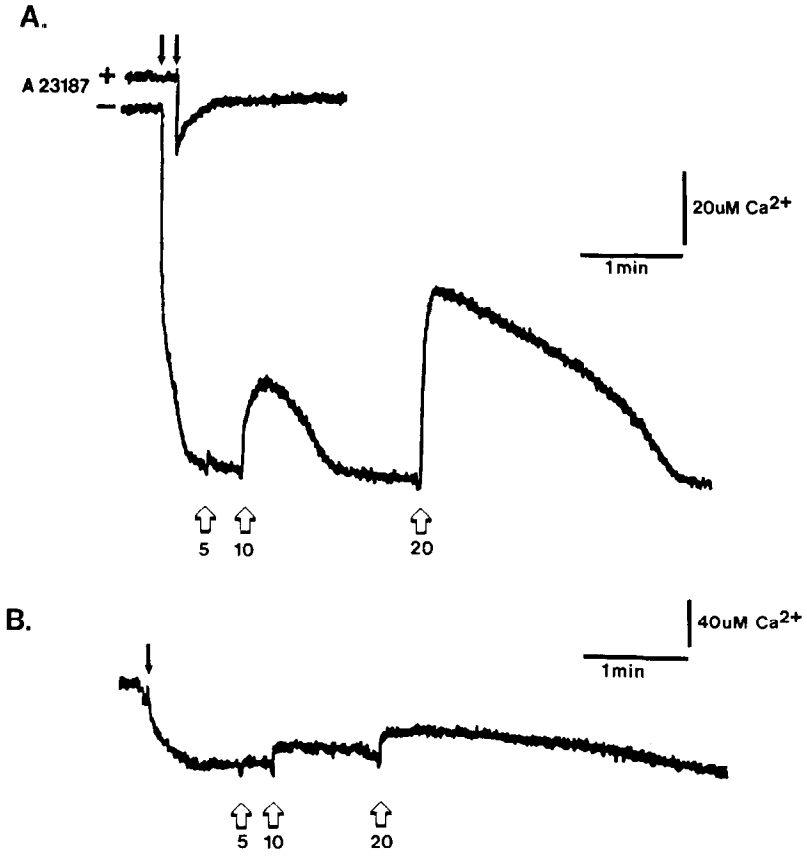

Figure 4: Effect of elevated Mg^{2+} upon Ca^{2+} uptake by HSR monitored as in Fig. 3A at 720-790nm. Assay conditions were as described in Fig. 3 except vesicles were pre-incubated in (A). 3mM Mg^{2+} in the presence (+) and absence (-) of 10μM A23187 and, (B). 9mM Mg^{2+} without A23187 treatment. Ca^{2+} uptake was initiated by 1mM Mg.ATP addition (solid arrows) in the presence of ATP regeneration (see Methods). Ca^{2+} release was induced by addition of 5, 10 and 20μM Ca^{2+} as indicated (open arrows). The horizontal and vertical bars denote scales for time and ΔCa^{2+} as indicated. The direction of Ca^{2+} uptake and release are as described in the legend to Fig. 3.

An alternate strategy that eliminates the ATP absorbance artifact at 720nm is the inclusion of excess Mg^{2+} (10mM) in assay media. This has been adopted when Murexide (24), Arsenazo III (25) and, Antipyrylazo III (11) were employed to monitor Ca^{2+} transients at the respective wavelength pairs. In view of the effects of elevated Mg^{2+} upon (a) HSR Ca^{2+} release (13) and (b) divalent cation:AP III difference spectra (Figs. 1 and 2) it was of interest to determine the general appropriateness of this strategy. As shown in Fig. 4A the absorbance artifact was significantly reduced when vesicles were pre-incubated in the presence of 3mM Mg^{2+} prior to addition of nucleotide and is completely eliminated at 10mM total Mg^{2+} (Fig. 4B). This effect is predicted by the spectral scans shown in Figs. 1C and 2C. However, loss of both the secondary and tertiary phases of uptake was also observed with elevated Mg^{2+}. This may reflect Mg^{2+} inhibition of Ca^{2+} release channel opening subsequent to the initial fast phase (see above) and probably accounts for Mg^{2+} stimulation of HSR Ca^{2+} uptake reported earlier (26,27). Additionally, Ca^{2+}-induced Ca^{2+} release was less sensitive to trigger Ca^{2+} (Fig. 4A). Ca^{2+} release was not triggered by 5μM free Ca^{2+} and 10μM free Ca^{2+} was required to minimally stimulate Ca^{2+} release. With 20μM free trigger Ca^{2+}, 25-30nmol $Ca^{2+}.mg^{-1}$ was released. Mg^{2+}, therefore, appears to decrease the Ca^{2+} sensitivity of Ca^{2+}-induced Ca^{2+} release in agreement with rapid kinetic studies of $^{45}Ca^{2+}$ release from passivley loaded HSR vesicles (28). A 60% reduction in the rate of Ca^{2+} re-uptake, after 20μM Ca^{2+} addition, was also observed when compared to the lower Mg^{2+} condition in Fig. 3 where the sum of added and released Ca^{2+} was comparable (~40-50nmol $Ca^{2+}.mg^{-1}$). At 10mM Mg^{2+} (Fig. 4B) the initial rate of Ca^{2+} uptake was much reduced and Ca^{2+}-induced Ca^{2+} release was completely abolished with a greatly extended re-uptake of added Ca^{2+}. These data indicate that Mg^{2+} may also inhibit Ca^{2+} channel closing subsequent to release, although we did not discriminate between this possibility and Ca^{2+}-ATPase inhibition (see ref 12). It was also evident that Mg^{2+} elevation decreased the sensitivity of measurement. Under the conditions defined by Fig. 3 at both wavelength pairs Δ10μM Ca^{2+} produced a ΔA of 0.0025 absorbance units. At 10mM total Mg^{2+} (inset Fig. 4) Δ50μM Ca^{2+} resulted in a ΔA of only 0.0024 absorbance units.

Clearly, elevation of assay Mg^{2+}, in order to eliminate ATP absorbance artifacts during dual-wavelength spectroscopy of Ca^{2+}:AP III ΔA changes, is an inappropriate general strategy for HSR Ca^{2+} transport studies. Selection of new wavelength pairs in accordance with the influence of ATP upon dye:ligand difference spectra (Fig. 2) facilitates study of HSR Ca^{2+} uptake and release at relatively high levels of ATP and intracellularly appropriate concentrations of Ca^{2+} and Mg^{2+}. In addition, resolution of initial rapid uptake of Ca^{2+} is improved without loss of measurement sensitivity.

Acknowledgments: Supported by NSERC and MRC, Canada. J.G. is a B.C. and Yukon Heart and Stroke Foundation Research Trainee.

REFERENCES

1. Endo, M. (1977) Physiol. Rev. 57, 71-108.
2. Gould, G.W., McWhirter, J.M., East, J.M., and Lee, A.G. (1987) Biochem. J. 245, 739-749.
3. Ohnishi, S.T. (1979) J. Biochem. (Tokyo) 86, 1147-1150.
4. Watras, J., and Katz, A.M. (1984) Biochem. Biophys. Acta. 769, 429-439.
5. Rubtsov, A.M., Smirnova, M.B., and Boldyrev, A.A. (1988) Biochem. Int. 17, 629-636.
6. Rubtsov, A.M., and Murphy, A.J. (1988) Biochem. Biophys. Res. Comm. 154, 462-468.
7. Trimm, J.L., Salama, G., and Abramson, J.J. (1986) J. Biol. Chem. 261, 16092-16098.
8. Morii, H., Takisawa, H., and Yamamoto, T. (1985) J. Biol. Chem. 260, 11536-11541.

9. Palade, P. (1987) J. Biol. Chem. 262, 6135-6141.
10. Palade, P. (1987) J. Biol. Chem. 262, 6142-6148.
11. Scarpa, A., Brinley, F.J., Dubyak, (1978) Biochemistry 17, 1378-1386.
12. McWhirter, J.M., Gould, G.W., East, J.M., and Lee, A.G. (1987) Biochem. J. 245, 731-738.
13. Meissner, G., and Henderson, J.S. (1987) J. Biol. Chem. 262, 3065-3073.
14. Scarpa, A. (1978) Methods Enzymol. 56, 301-338.
15. Kendrick, N.C., Ratzlaff, R.W., and Blaustein, M.P. (1977) 83, 433-450.
16. Rios, E., and Schneider, M.F. (1981) Biophys. J. 36, 607-621.
17. Abramcheck, C.W., and Best, P.M. (1989) J. Gen. Physiol. 93, 1-21
18. Inui, M., Saito, A., and Fleischer, S. (1987) J. Biol. Chem. 262, 1740-1747.
19. Lowry, O.H., Rosenbrough, N.J., Farr, A.L., and Randall, R.J. (1951) J. Biol. Chem. 193, 265-275.
20. Fabiato, A. (1981) J. Gen. Physiol. 78, 457-497.
21. Baylor, S.M., Chandler, W.K., and Marshall, M.W. (1982) J. Physiol. (Lond.) 331, 139-177.
22. Ikemoto, N., Ronjat, M., and Meszaros, L.G. (1989) J. Bioenerg. Biomembr. 247-266.
23. Ikemoto, N., and Koshita, M. (1988) Biophys. J. 53, 421a.
24. Inesi, G., and Scarpa, A. (1972) Biochemistry 11, 356-359.
25. Herbette, L., Scarpa, A., Blaisie, J.K., Bauer, D.R., Wang, C.T., and Fleischer, S. (1981) Biophys. J. 36,27-46.
26. Watras, J. (1985) Biochim. Biophys. Acta. 812, 333-344.
27. Chu, A., Volpe, P., Costello, B., and Fleischer, S. (1986) Biochemistry 25, 8315-8324.
28. Meissner, G., Darling, E., and Eveleth, J. (1986) Biochemistry 25, 236-244.